PROCEEDINGS OF SCIENCE

The latest CMS results on Higgs boson decaying to two photons with 13 TeV data

Michael Planer[*†]
University of Notre Dame (US)
E-mail: michael.david.planer@cern.ch

The latest results of the measurement of the Higgs boson decaying into two photons with the full 2016 data will be presented. The analysis is performed using the dataset recorded by the CMS experiment at the LHC from pp collisions at centre-of-mass energies of 13 TeV corresponding to an integrated luminosity of 35.9 fb^{-1}.

The European Physical Society Conference on High Energy Physics
5-12 July
Venice, Italy

[*]Speaker.
[†]On behalf of the CMS Collaboration.

PoS(EPS-HEP2017)328

1. Introduction

Experimental data at low and high energies are well explained by the standard model (SM) [1] [2] [3]. One of the most recent validations of the SM came from Run 1 at the LHC when a new particle consistent with the SM Higgs boson [6] [7] [8] was discovered by ATLAS [5] and CMS [4]. One of the most prominent channels used to discover the Higgs boson was the H$\rightarrow \gamma\gamma$. The clean final state and well resolved mass peak help to overcome the low branching ratio and make this channel one of the most significant.

The latest measurements of properties of the Higgs boson in the H$\rightarrow \gamma\gamma$ channel are presented [9]. They include the signal strength for different production modes, the effective coupling to fermions and bosons, and the effective coupling to photons and gluons. An integrated luminosity of 35.9 fb^{-1} at $\sqrt{s} = 13$ TeV was recorded by the CMS detector during the 2016 LHC run period in proton-proton collisions and is used in this analysis. Event categories are designed to select the Higgs production modes: vector boson fusion (VBF), associated production with a vector boson (WH, ZH), associated production with a top quark pair (ttH), as well as gluon-gluon fusion (ggH).

2. Analysis Strategy

The H$\rightarrow \gamma\gamma$ analysis searches for events which have two high p_T photons with an invariant mass between 100 and 180 GeV. In this range there is a large irriducible background from QCD production of two photons as well as a reducible background from one or more misidentified jet fragments producing a photon candidate. With precise mass-resolution, the Higgs mass peak can be seen above the smooth background mass distribution.

In order to reduce the background from fake photons, a boosted decision tree (BDT) is trained to separate prompt photons from candidates coming from misidentified jet fragments. The performance of this BDT can be seen in the left figure 1. The largest contributor to the experimental width of the Higgs boson mass peak comes from the photon energy resolution measurement. The energy is corrected using a sample of Z$\rightarrow e^+e^-$ events where the electrons shower similarly to photons. The diphoton mass peaks after the energy corrections can be seen in figure 2.

If the vertex position is incorrectly measured by more than 1cm this has a larger effect on the Higgs mass resolution than the energy resolution of the photon. A BDT was trained to choose the correct vertex; inputs to the BDT are related to the track recoil against the diphoton system. The vertex is reconstructed within 1cm of the true vertex in 80% of events selected by this analysis as shown in the right figure 1.

Events are classified according to Higgs production mechanism, according to their mass resolution, and according to their sensitivity. A BDT was trained as an estimate of a per-event diphoton mass resolution. Figure 3 shows the separation power of the diphton BDT. Events are split into 14 categories in the following order: ttHLeptonic, ttHHadronic, ZHLeptonic, WHLeptoinc, VHLeptonicLoose, 3 VBF-tagged categories, VHMET, VHHadronic, and 4 Untagged categories. Various requirement based on kinematic properties of the diphoton pair as well as additional objects in the event were used in this categorization. Parametric models for signal and background were built separately for each category. The signal models are built using simulated signal samples, taking

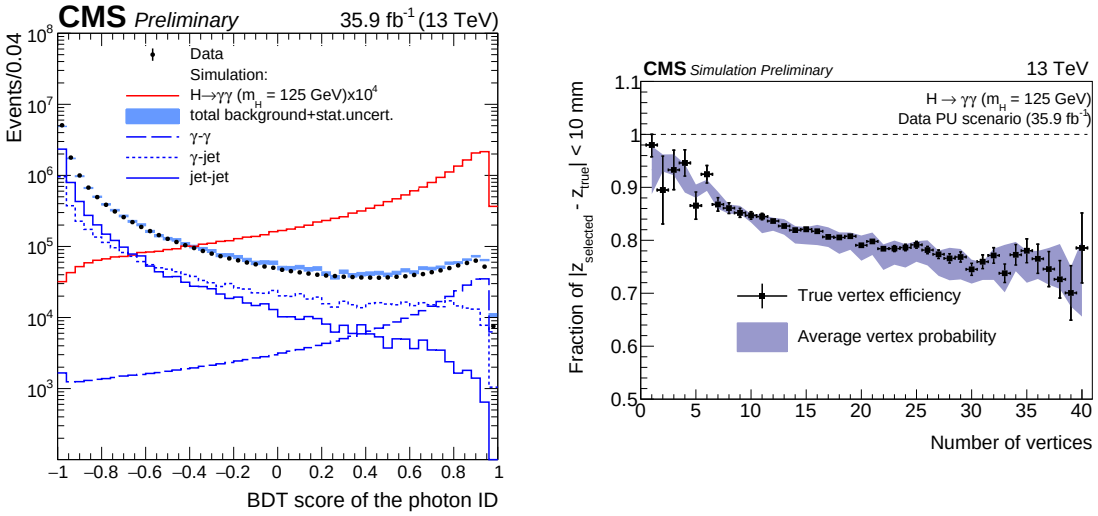

Figure 1: Left: Photon identification BDT score of the lower-scoring photon of diphoton pairs with an invariant mass in the range $100 < m_{\gamma\gamma} < 180$ GeV, for events passing the preselection in the 13 TeV data set (points), and for simulated background events (blue histogram). Histograms are also shown for different components of the simulated background. The sum of all background distributions is scaled up to data. The red histogram corresponds to simulated Higgs boson signal events. Right: Comparison of the true vertex identification efficiency and the average estimated vertex probability as a function of the number of primary vertices in simulated H$\rightarrow \gamma\gamma$ events with $m_H = 125$ GeV. Events are weighted according to the cross sections of the different production modes and to match the distributions of pileup and location of primary vertices in data. [9]

into account correction and scale factors. The background models are taken from data where a nuisance parameter varies over a set of possible functional forms [10].

3. Results

The diphoton invariant mass distribution, reconstructed using the techniques described in the previous section, is shown in the left figure 4. The right figure 4 corresponds to the expected yields from simulation described in the previous section. The left figure 5 shows the signal strength of the Higgs boson compared to the standard model for the ggH, ttH, VBF, and VH production modes. The cross section ratios for each process in the minimal Higgs Simplified Template Cross Section (STXS) framework from the CERN Yellow Report 4 of LHC-HXSWG [11] are shown in the right figure 5. Figures 6 give the best fit value for signal strength μ for m_H profiled $\mu = 1.16^{+0.15}_{-0.14} = 1.16^{+0.11}_{-0.10}(\text{stat.})^{+0.09}_{-0.08}(\text{sys.})^{+0.06}_{-0.05}(\text{theo.})$. The right plot from this figure shows the best fit signal strength for the ggH and ttH production vs the VBF and VH production mechanism. The best fit values are: $\mu_{ggH,ttH} = 1.19^{+0.20}_{-0.18}$ and $\mu_{VBF,VH} = 1.01^{+0.57}_{-0.51}$.

Two dimensional likelihood scans of the coupling modifiers to the Higgs boson are presented in figure 7. The left plot shows the coupling modifiers to fermions and bosons (assuming universality among fermions and bosons) while the right plot shows the coupling to gluons and photons

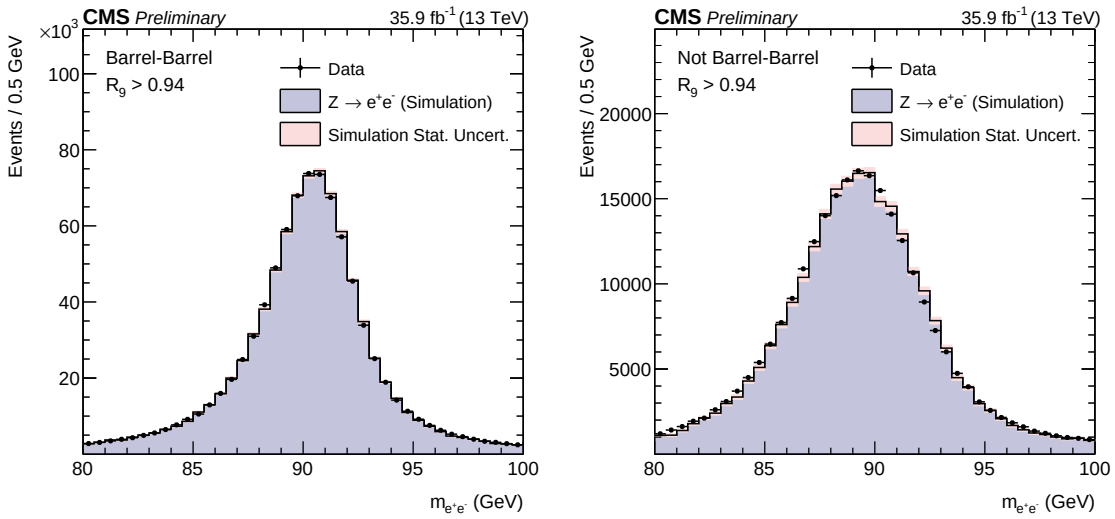

Figure 2: Comparison of the dielectron invariant mass distributions in data and simulation (after energy smearing) for Z$\rightarrow e^+e^-$ events where electrons are reconstructed as photons. The comparison is shown requiring R9$>$ 0.94 for both photons and for (Left) events with both showers in the barrel, and (Right) the remaining events. The simulated distribution is normalized to the integral of the data distribution in the range 87 GeV$<m_{e^+e^-}<$93 GeV. [9]

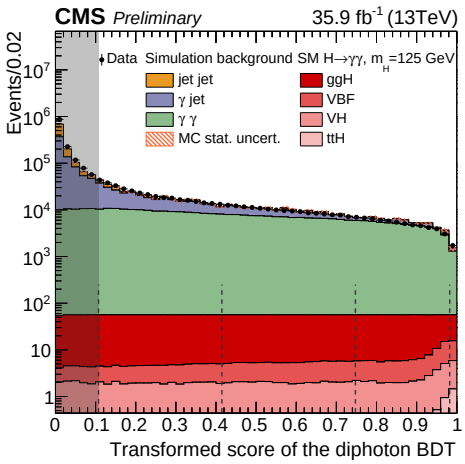

Figure 3: Transformed score of the diphoton multivariate classifier for events with two photons satisfying the preselection requirements in data (points), simulated signal (red shades), and simulated background (coloured histograms). Both signal and background are stacked together. The vertical dashed lines show the boundaries of the untagged categories, the grey shade indicates events discarded from the analysis. [9]

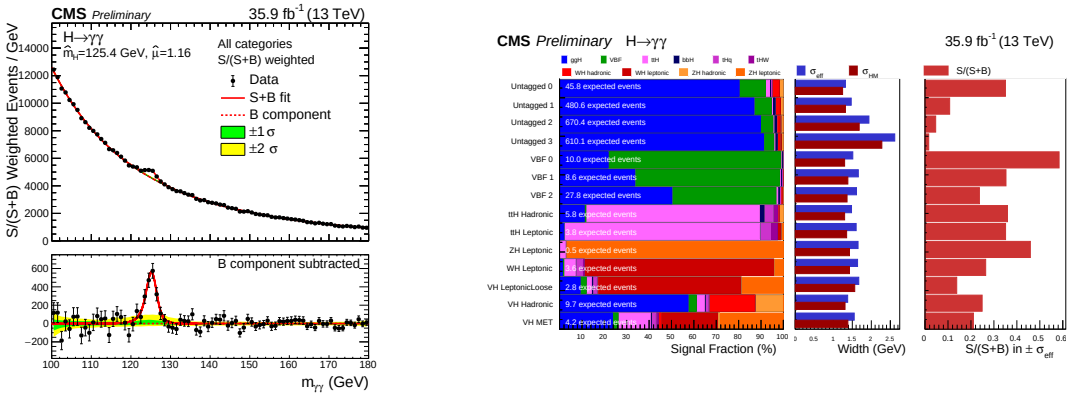

Figure 4: Left: Data points (black) and signal plus background model fits for all categories summed and weighted by their sensitivity (Left). The one standard deviation (green) and two standard deviation bands (yellow) include the uncertainties in the background component of the fit. The bottom plot shows the residuals after background subtraction. Right: Expected fraction of signal events per production mode in the different categories. For each category, the σ_{eff} and σ_{HM} of the signal model are given, as described in the text. The ratio of the number of signal events (S) to the number of signal plus background events (S+B) is shown on the right hand side. [9]

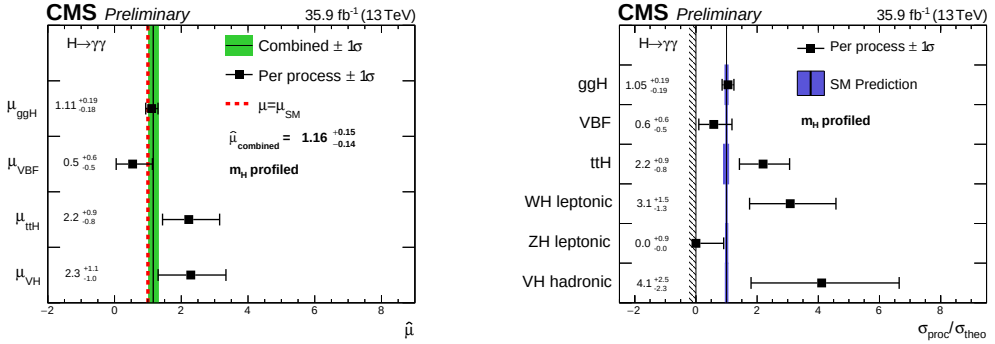

Figure 5: Left: Signal strength modifiers measured for each process (black points) for profiled m_H, compared to the overall signal strength (green band) and to the SM expectation (dashed red line). Right: Cross section ratios measured for each process (black points) in the Higgs Simplified Template Cross Section framework, for profiled m_H, compared to the SM expectation and its uncertainties (green band). The signal strength modifiers are constrained to be non-negative, as indicated by the vertical line and hashed pattern at zero. [9]

with 1σ and 2σ contours. Each of the coupling constants is shown relative to the SM expectations. The measured coupling constants are consistent with the standard model prediction.

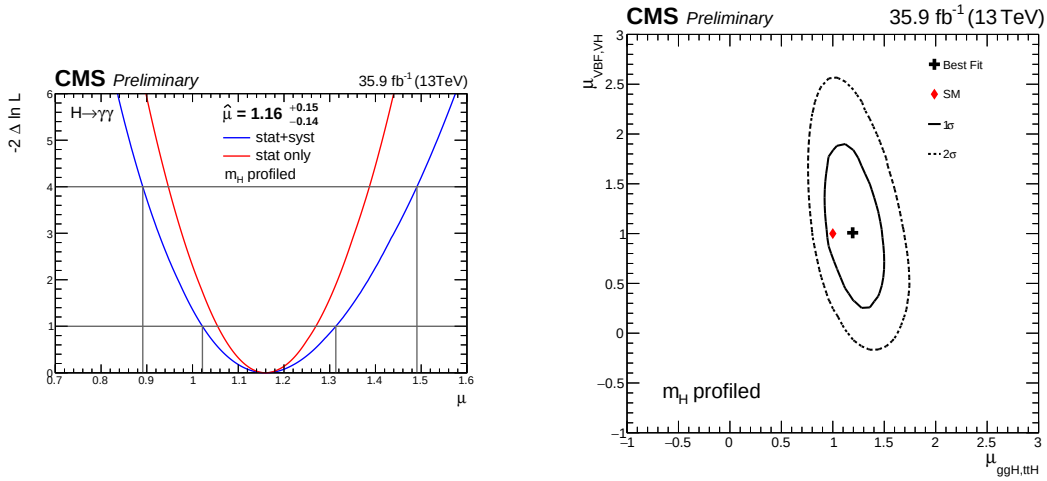

Figure 6: Left: The likelihood scan for the signal strength where the value of the standard model Higgs boson mass is profiled in the fit. Right: The two-dimensional best-fit (black cross) of the signal strengths for fermionic (ggH, ttH) and bosonic (VBF, ZH, WH) production modes compared to the SM expectations (red diamond). The Higgs boson mass is profiled in the fit. The solid (dashed) line represents the 1 (2) standard deviation confidence region. [9]

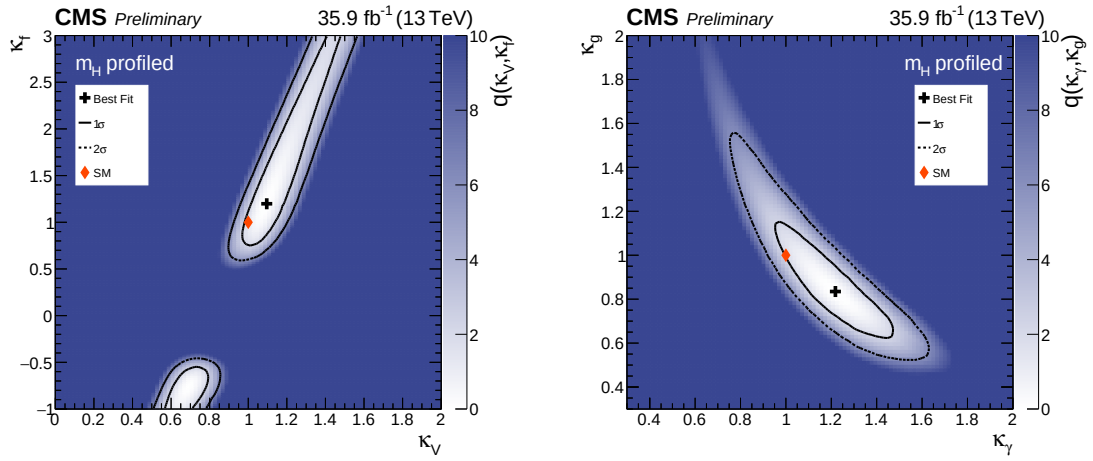

Figure 7: Two-dimensional likelihood scans of κ_γ versus κ_V (Left) and κ_g versus κ_γ (Right). All four variables are expressed relative to the SM expectations. The mass of the Higgs boson is profiled in the fits. The crosses indicate the best-fit values, the diamonds indicate the Standard Model expectations. [9]

References

[1] S. L. Glashow, Nucl. Phys. **22** (1961) 579. doi:10.1016/0029-5582(61)90469-2

[2] S. Weinberg, Phys. Rev. Lett. **19** (1967) 1264. doi:10.1103/PhysRevLett.19.1264

[3] A. Salam, Conf. Proc. C **680519** (1968) 367.

[4] S. Chatrchyan et al. [CMS Collaboration], Phys. Lett. B **716** (2012) 30 doi:10.1016/j.physletb.2012.08.021 [arXiv:1207.7235 [hep-ex]].

[5] G. Aad et al. [ATLAS Collaboration], Phys. Lett. B **716** (2012) 1 doi:10.1016/j.physletb.2012.08.020 [arXiv:1207.7214 [hep-ex]].

[6] F. Englert and R. Brout, Phys. Rev. Lett. **13** (1964) 321. doi:10.1103/PhysRevLett.13.321

[7] P. W. Higgs, Phys. Rev. Lett. **13** (1964) 508. doi:10.1103/PhysRevLett.13.508

[8] G. S. Guralnik, C. R. Hagen and T. W. B. Kibble, Phys. Rev. Lett. 13 (1964) 585. doi:10.1103/PhysRevLett.13.585

[9] CMS Collaboration, CMS-PAS-HIG-16-040, http://cds.cern.ch/record/2264515.

[10] P. D. Dauncey, M. Kenzie, N. Wardle and G. J. Davies, JINST **10** (2015) no.04, P04015 doi:10.1088/1748-0221/10/04/P04015 [arXiv:1408.6865 [physics.data-an]].

[11] D. de Florian et al. [LHC Higgs Cross Section Working Group], doi:10.23731/CYRM-2017-002 arXiv:1610.07922 [hep-ph].